Simulation of Molten Salt Reactors with Moltres

Andrei Rykhlevskii[1], Alexander Lindsay[2], Kathryn Huff[1]
Advanced Reactors and Fuel Cycles Group

[1]University of Illinois at Urbana-Champaign

[2]Idaho National Laboratory

Feb 26, 2019

ILLINOIS

Outline

Advanced Reactors and Fuel Cycles group (PI: Kathryn Huff)

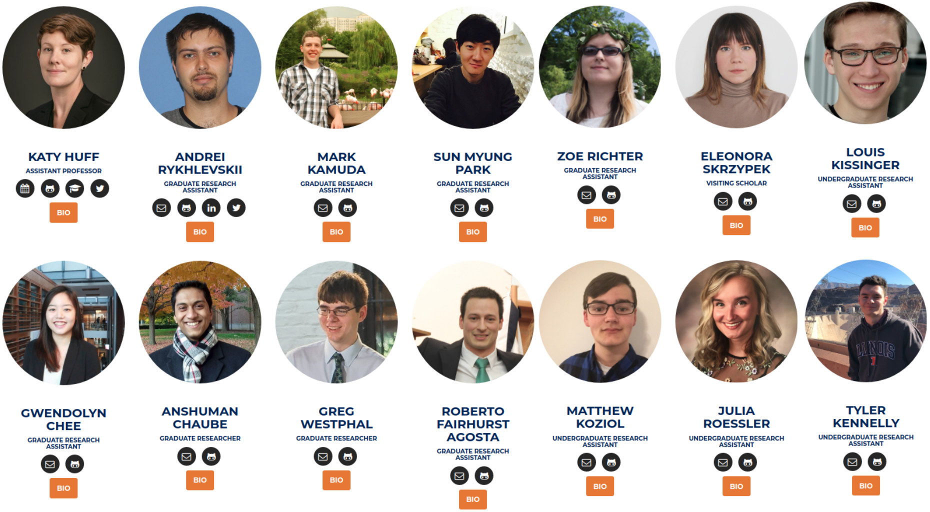

Figure 1: Current Advanced Reactors and Fuel Cycles Group researchers.

Advanced Reactors and Fuel Cycles group (PI: Kathryn Huff)

Figure 2: Past ARFC Group members who contributed to this work.

Molten Salt Reactor Types

Stationary Fuel

1. Graphite block with TRISO fuel, clean salt works as coolant (e.g. TMSR-SF1, FHR-DR)
2. Plate Fuel: hexagonal fuel assembly is similar in shape to a typical sodium-cooled reactor

Mobile Fuel

1. Mobile solid fuel elements (e.g. pebbles) cooled by clean salt (e.g. PB-FHR)
2. Non-circulating liquid fuel salt (e.g. TerraPower MCFR)
3. **Circulating fuel salt** which also works as coolant (e.g. Molten Salt Reactor Experiment (MSRE), Molten Salt Breeder Reactor (MSBR), TAP MSR)

Stationary and Mobile Solid fuel

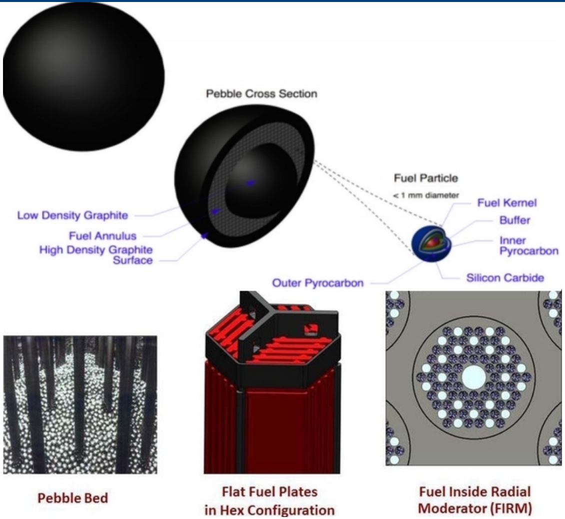

Figure 3: TRISO fuel particle (top) and FHR fuel designs (bottom). Source [1].

Mobile, Non-Circulating, Liquid Fuel

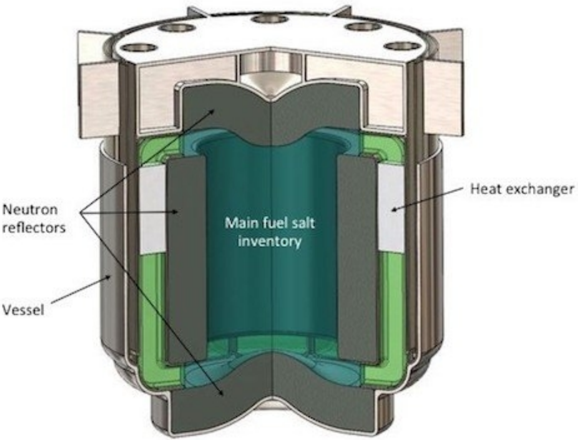

Figure 4: The TerraPower MCFR is an example of reactor design with **liquid, mobile, non-circulating** chloride salt fuel. Source [2].

Mobile, Circulating, Liquid Fuel

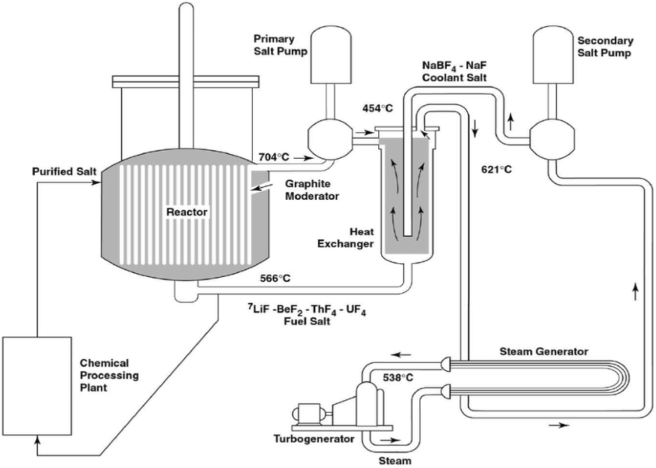

Figure 5: The MSBR is an example of reactor design with **liquid, mobile, circulating** fluoride salt fuel [3].

Why Molten Salt Reactors with circulating fuel?

Main advantages of liquid-fueled Molten Salt Reactors (MSRs) [4]

1. High coolant temperature (600-750°C)
2. Fuel diversity (^{235}U, ^{233}U, Thorium, U/Pu)
3. Increased inherent safety
4. High fuel utilization $\Rightarrow$ less nuclear waste generated
5. Online reprocessing and refueling
6. Thermal/epithermal (MSBR) or fast spectrum (Molten Salt Fast Reactor (MSFR))
7. Can produce more fissile material than it consumes (breeder)
8. Nuclear Spent Fuel Transmuter (e.g. REBUS-3700 [5], MOSART [6])

Challenges in MSR Simulation

1. Contemporary burnup codes cannot treat fuel movement
2. Neutron precursor location is hard to estimate
3. Operational and safety parameters change during reactor operation
4. Power generation strongly depends on fuel temperature and vica versa

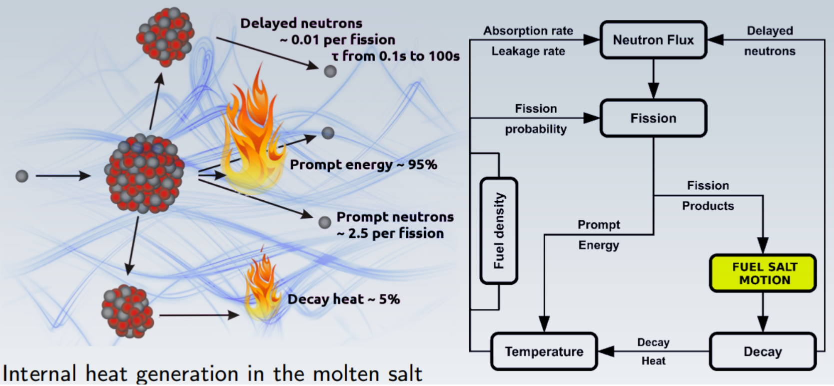

Figure 6: Challenges in simulating MSRs (Image courtesy of Manuele Aufiero,2012).

Research objectives

Multiphysics simulation of MSR (Moltres/MOOSE)[7]

1. Demonstrate steady-state and transient coupling of neutron fluxes, precursor drift, and thermal-hydraulics
2. Implement advective movement of delayed neutron precursors
3. Demonstrate capabilities with 2D axisymmetric and 3D mesh
4. Simple transients: change of flow and moderator movement

Outline

Acquiring Moltres

```
git clone https://github.com/arfc/moltres
cd moltres
git submodule init
git submodule update
```

Moltres (coupling in MOOSE)

Moltres principal concept [7]

- Moltres is built on top of the Multi-physics Object-Oriented Simulation Environment (MOOSE)
- MOOSE interfaces with libMesh to discretize simulation volume into finite elements
- Provides interface for coding residuals that correspond to weak form of governing PDEs; also interface for coding Jacobians ⇒ more accurate Jacobians ⇒ more efficient convergence
- Residuals and Jacobians send to PetSc which handles solution of resulting non-linear system of algebraic equations

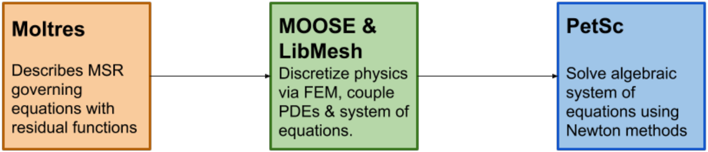

Figure 7: Moltres principal scheme

Intro to Moltres

- Liquid-fueled, molten salt reactors
- Multi-group diffusion (arbitrary number of groups)
- Advective movement of delayed neutron precursors
- Reynolds-averaged Navier-Stokes thermal hydraulics
- 2D axisymmetric
- 3D unstructured or structured

Moltres Kernels

Typical symbols (e.g. $\phi =$ neutron flux, $T =$ temperature, and $C =$ precursor concentrations).

CoupledFissionEigenKernel

$$\frac{\chi_g^p}{k}\sum_{g'=1}^{G}(1-\beta)\nu\Sigma_{g'}^{f}\phi_{g'}$$

CoupledFissionKernel

$$\chi_g^p\sum_{g'=1}^{G}(1-\beta)\nu\Sigma_{g'}^{f}\phi_{g'}$$

CoupledScalarAdvection

$$\nabla\cdot\vec{a}u$$

DelayedNeutronSource

$$\chi_g^d\sum_{i}^{I}\lambda_i C_i$$

DivFreeCoupledScalarAdvection

$$\vec{a}\cdot\nabla u$$

Moltres Kernels

FissionHeatSource

$$\frac{P}{\int_{\partial V} \sum_{g'=1}^{G} \nu \Sigma_{g'}^{f} \phi_{g'} \, dV} \sum_{g'=1}^{G} \nu \Sigma_{g'}^{f} \phi_{g'}$$

GammaHeatSource

$$\gamma Q_f$$

$\gamma =$ moderator heat dissipation by gamma and neutron irradiation

$$Q_f = \sum_{g=1}^{G} \epsilon_{f,g} \Sigma_{f,g} \phi_g$$

$\epsilon_{f,g} =$ heat per fission event.

GroupDiffusion

$$\nabla \cdot D_g \nabla \phi_g$$

Moltres Kernels

InScatter

$$\sum_{g \neq g'}^{G} \Sigma_{g' \to g}^{s} \phi_{g'}$$

NtTimeDerivative

$$\frac{1}{v_g} \frac{\partial \phi_g}{\partial t}$$

PrecursorDecay

$$\lambda_i C_i$$

PrecursorSource

$$\sum_{g'=1}^{G} \beta_i \nu \Sigma_{g'}^{f} \phi_{g'}$$

ScalarAdvectionArtDiff

$$\nabla \cdot -\delta \nabla u$$

$\delta =$ artificial diffusion coefficient

Moltres Kernels

ScalarTransportTimeDerivative

$$\frac{\partial u}{\partial t}$$

SelfFissionEigenKernel

$$\frac{-\nu_f \Sigma_f \phi}{k}$$

SigmaR

$$\Sigma_g^r \phi_g$$

TransientFissionHeatSource

$$\sum_{g=1}^{G} \epsilon_{f,g} \Sigma_{f,g} \phi_g$$

Governing Equations

Time-dependent multi-group diffusion

$$\frac{1}{v_g}\frac{\partial \phi_g}{\partial t} - \nabla \cdot D_g \nabla \phi_g + \Sigma_g^r \phi_g = \sum_{g \neq g'}^{G} \Sigma_{g' \to g}^s \phi_{g'} + \chi_g^p \sum_{g'=1}^{G} (1-\beta)\nu \Sigma_{g'}^f \phi_{g'} + \chi_g^d \sum_{i}^{I} \lambda_i C_i$$

v_g = speed of neutrons in group g
ϕ_g = flux of neutrons in group g
t = time
D_g = Diffusion coefficient for neutrons in group g
Σ_g^r = macroscopic cross-section for removal of neutrons from group g
$\Sigma_{g' \to g}^s$ = macroscopic cross-section of scattering from g' to g
χ_g^p = prompt fission spectrum, neutrons in group g
G = number of discrete groups, g
ν = number of neutrons produced per fission
Σ_g^f = macroscopic cross section for fission due to neutrons in group g
χ_g^d = delayed fission spectrum, neutrons in group g
I = number of delayed neutron precursor groups
β = delayed neutron fraction
λ_i = average decay constant of delayed neutron precursors in precursor group i
C_i = concentration of delayed neutron precursors in precursor group i.

Governing Equations (2)

Delayed neutron precursors

$$\frac{\partial C_i}{\partial t} = \sum_{g'=1}^{G} \beta_i \nu \Sigma_{g'}^{f} \phi_{g'} - \lambda_i C_i - \frac{\partial}{\partial z} u C_i$$

Heat conduction-convection with fission source in fuel

$$\rho_f c_{p,f} \frac{\partial T_f}{\partial t} + \nabla \cdot \left(\rho_f c_{p,f} \vec{u} \cdot T_f - k_f \nabla T_f \right) = Q_f$$

ρ_f = density of fuel salt
$c_{p,f}$ = specific heat capacity of fuel salt
T_f = temperature of fuel salt
$\vec{u}$ = velocity of fuel salt
k_f = thermal conductivity of fuel salt
Q_f = source term = $\sum_{g=1}^{G} \epsilon_{f,g} \Sigma_{f,g} \phi_g$

Heat conduction with option for irradiation source in moderator

$$\rho_g c_{p,g} \frac{\partial T_g}{\partial t} + \nabla \cdot \left(-k_g \nabla T_g \right) = Q_g$$

ρ_g = density of graphite moderator
$c_{p,g}$ = specific heat capacity of graphite moderator
T_g = temperature of graphite moderator
k_g = thermal conductivity of graphite moderator
Q_g = source term in graphite moderator

Moltres MSRE Simulations

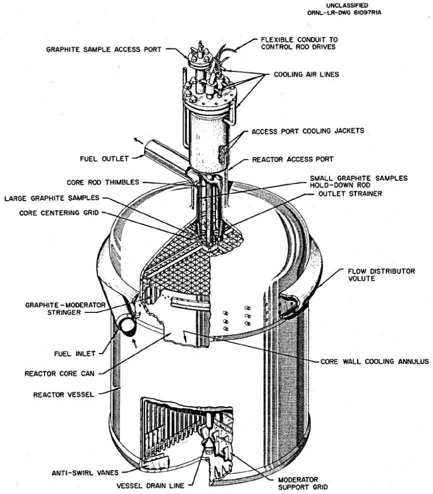

Fig. 6. MSRE Reactor Vessel.

Outline

Multiphysics simulation results (2D)

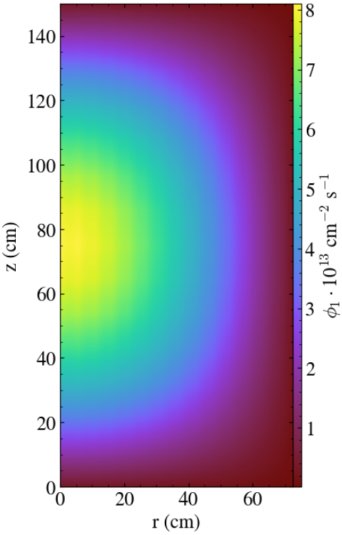

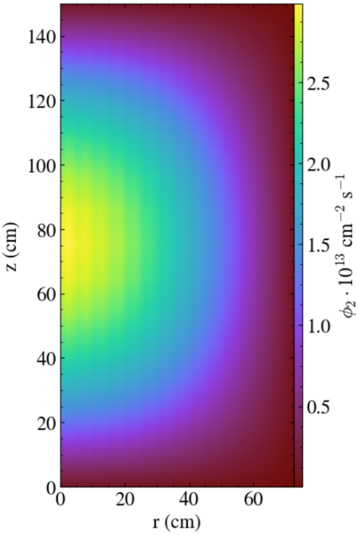

Multiphysics simulation results (2D) (2)

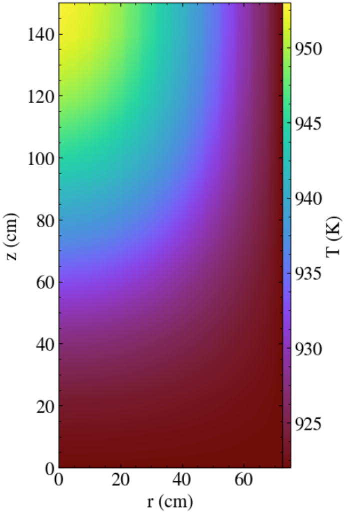

Figure 9: Temperature in channel obtained using Moltres [7].

Moltres vs MSRE Comparison

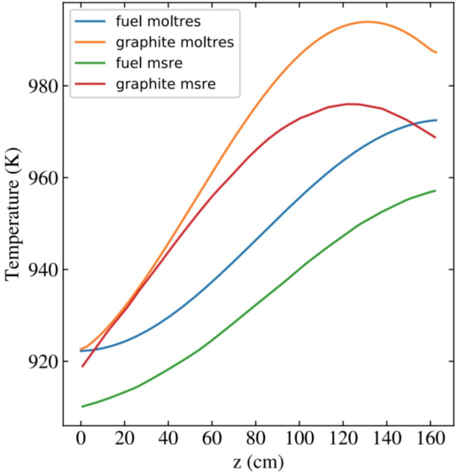

Fig. 11. Moltres and MSRE design (Briggs, 1964, p. 99) predicted axial temperature profiles in hottest channel and adjacent graphite.

Moltres vs MSRE Comparison (2)

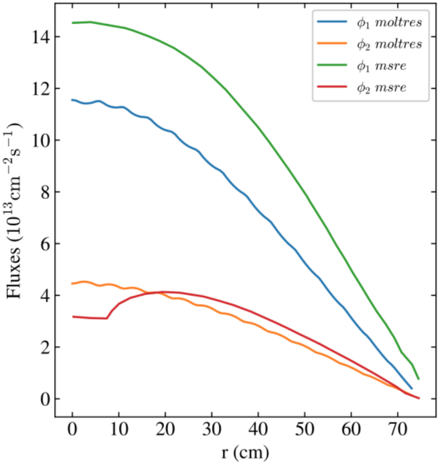

Fig. 12. The thermal and fast flux profiles at the core mid-plane ($z = H/2$) for the Moltres 2-D cylindrical axisymmetric model and the MSRE design model (Briggs, 1964, p. 92) ($r = 0$ is radial center of core).

Moltres vs MSRE Comparison (3)

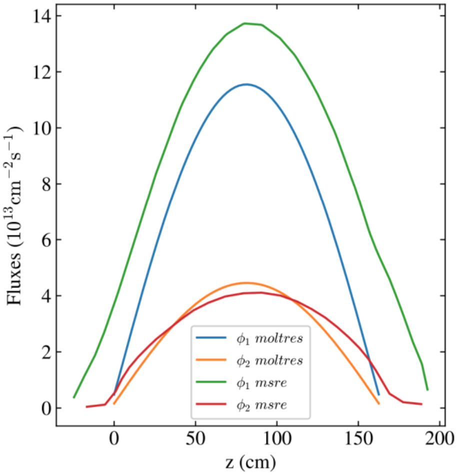

Fig. 13. Moltres axial flux profiles along the core center line and MSRE design axial flux profiles 21.336 cm (8.4 inches) from the core center line (Briggs, 1964, p. 91).

Multiphysics simulation results (3D)

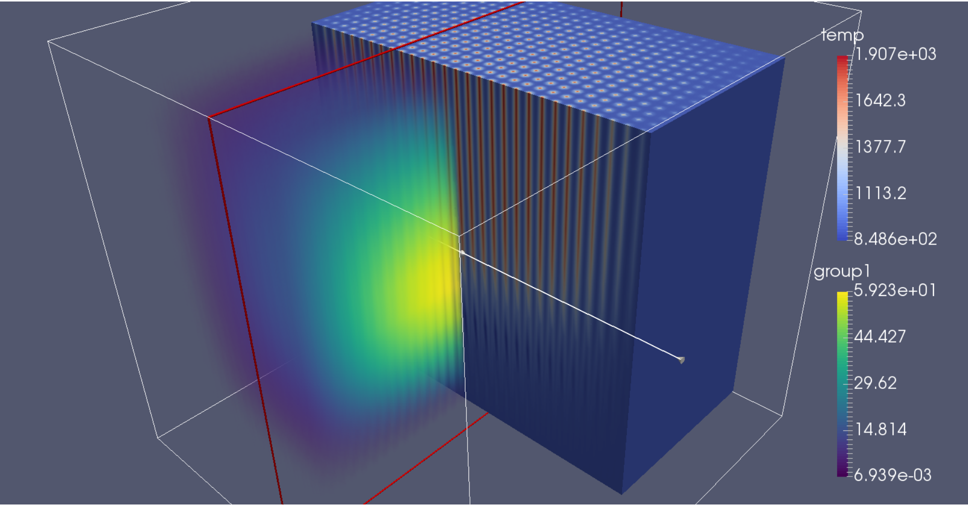

Figure 10: MSRE steady-state temperature and fast neutron flux [8].

Scaling on Blue Waters

Blue Waters:

- XK7 nodes (two AMD 6276 Interlagos CPU per node)
- 16 floating-point bulldozer core units per node or 32 ”integer” cores per node
- nominal clock speed is 2.45 GHz

Intra-Node Strong Scaling

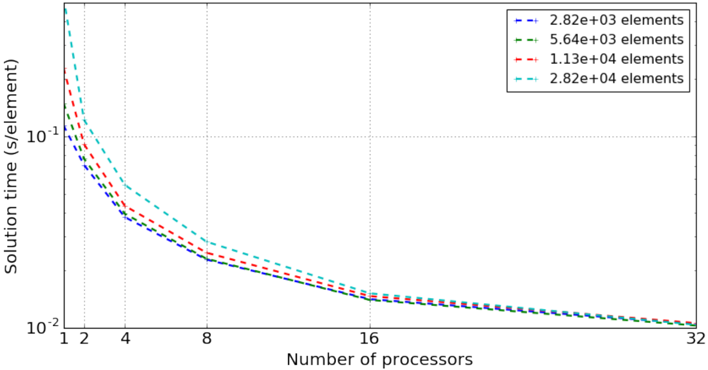

Figure 11: Moltres intra-node strong scaling efficiency for various problem sizes, for $n_{cores} \in [1, 32]$. Up to 8 cores, larger problems required considerably more time per element because of cache overhead. However, beyond 8 cores, scaling demonstrates asymptotic dependence on the number of processors due to increasing communication costs. The best parallel efficiency for the intra-node study is approximately 89%, achieved for the largest problem (28,200 elements).

Extra-node Strong Scaling

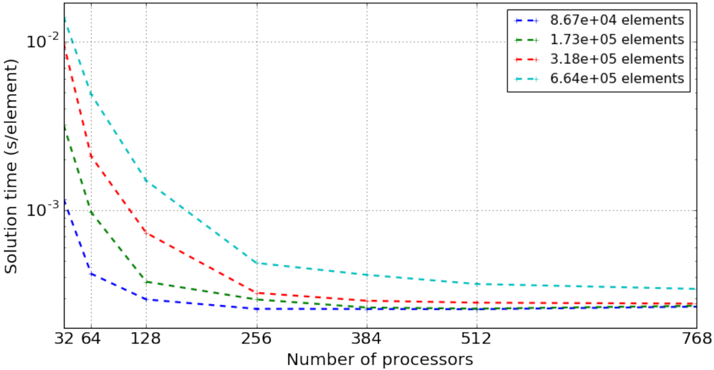

Figure 12: Moltres extra-node strong scaling efficiency for various problem sizes, for $n_{nodes} \in [1, 24]$. This takes into account communication costs between nodes. Cache overhead causes performance slow down for larger problems. Beyond 256 cores, simulation time per element remains almost constant for small cases (86,655 and 173,310 elements) and slighly decreases for the two larger problems. Parallel efficiency also grows with the problem size and reaches an optimal value of 73% for 664,355 elements.

Intra-node Weak Scaling

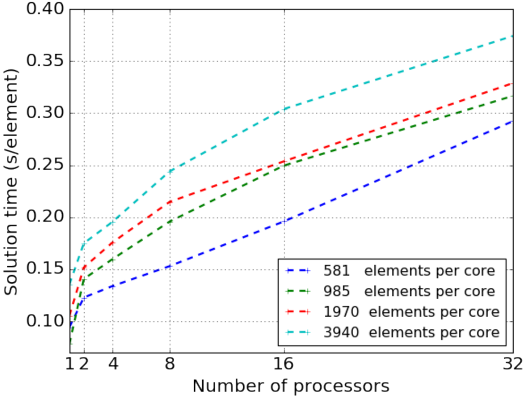

Figure 13: Weak scaling, in seconds per element vs. number of processors, for a constant number of elements per processor, and $n_{cores} \in [1, 32]$. Largest drop in performance occurs when the number of cores increases from one to ≈ 8, which corresponds to switching from no communication to a 2-D domain decomposition. Further reduction in performance of only about 50% over a range of 32 cores is likely caused by increased communication latency appearing from collective MPI calls.

Extra-node Weak Scaling

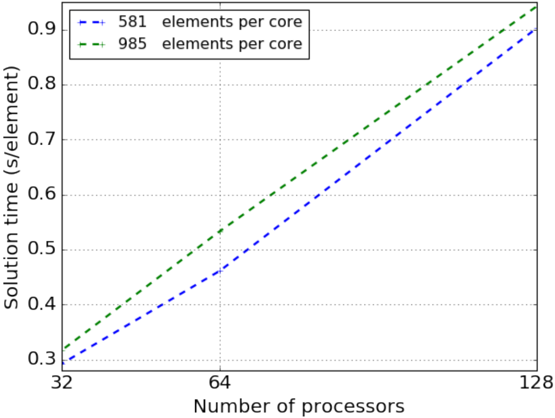

Figure 14: Weak scaling performance of Moltres on Blue Waters, in seconds per element vs. number of processors, for a constant number of elements per processor and $n_{cores} \in [32, 128]$. Performance drops by a factor of three, likely due to poor node selection by the Blue Waters job scheduler, increased latency and bandwidth costs.

Scaling Conclusions

Moltres scalability study results clearly indicate:

- Parallelization using LibMesh's automatic domain decomposition is great, but not perfectly efficient.
- This scaling performance is satisfactory for MSR simulations approached thus far.
- Moltres is memory-bound and therefore very sensitive to host memory and memory bandwidth.

Outline

Conclusions

Moltres

- Multiphysics Object-Oriented Simulation Environment (MOOSE) application developed at University of Illinois at Urbana-Champaign (UIUC) in the Advanced Reactors and Fuel Cycles (ARFC) group by lead developer Dr. Alexander Lindsay
- Neutron flux modeled with multigroup diffusion
- Delayed neutron precursor drift is incorporated
- Alongside fuel advection
- Gamma heating
- 2D-axisymmetric and 3D multiphysics results are presented
- Demonstrated strong parallel scaling (up to 384 physical cores)
- Further optimization is required for improved scaling.

Ongoing work

Demonstration & Verification

1. Verifying models of various MSR types with results generated by custom multiphysics models (using COMSOL, OpenFOAM, etc.)
   - Molten Salt Fast Reactor
   - Transatomic Power
   - Molten Salt Breeder Reactor
   - etc.
2. Demonstrating Moltres capabilities for various transients and operational behavior:.
   - load following
   - Loss of Forced Cooling
   - Loss of Heat Sink
   - Reactivity-Initiated Accident
   - etc.

Future work

Thermal Hydraulics Extensions

Realistic thermal hydraulics will enable more realistic precursor drift. Current efforts seek to incorporate:

1. Realistic natural circulation (better than Boussinesq approximation)
2. Insights from Computational Fluid Dynamics (CFD) regarding laminar-turbulent transitional flow behavior (e.g. Nek5000 [9])
3. Fuel salt compressibility (as shown in Aufiero et al. [10]).
4. Fuel composition as a coupled variable.

Acknowledgement

- This research is part of the Blue Waters sustained-petascale computing project, which is supported by the National Science Foundation (awards OCI-0725070 and ACI-1238993) and the state of Illinois.
- Andrei Rykhlevskii is supported by the Department of Nuclear, Plasma, and Radiological Engineering.
- Kathryn Huff is additionally supported by the NRC Faculty Development Program, the NNSA (awards DE-NA0002576 and DE-NA0002534), and the International Institute for Carbon Neutral Energy Research (WPI-I2CNER).
- The authors would like to thank members of Advanced Reactors and Fuel Cycles research group (ARFC) at the University of Illinois at Urbana Champaign who provided valuable code reviews and proofreading.
- Alex Lindsay (Idaho National Laboratory), Gavin Ridley (Yellowstone Energy), Alvin Lee, Tomasz Kozlowski (University of Illinois)

References I

[1] Charles Forsberg and Per F. Peterson.
Basis for Fluoride Salt-Cooled High-Temperature Reactors with Nuclear Air-Brayton Combined Cycles and Firebrick Resistance-Heated Energy Storage.
Nuclear Technology, 196(1):13–33, October 2016.

[2] DOENE.
Southern Company and TerraPower Prep for Testing on Molten Salt Reactor, August 2018.

[3] M. W. Rosenthal, P. R. Kasten, and R. B. Briggs.
Molten-Salt Reactors - History, Status, and Potential.
Nuclear Applications and Technology, 8(2):107–117, February 1970.

[4] Badawy M. Elsheikh.
Safety assessment of molten salt reactors in comparison with light water reactors.
Journal of Radiation Research and Applied Sciences, 6(2):63–70, October 2013.

[5] A. Mourogov and P. M. Bokov.
Potentialities of the fast spectrum molten salt reactor concept: REBUS-3700.
Energy Conversion and Management, 47(17):2761–2771, October 2006.

References II

[6] V. Ignatiev, O. Feynberg, I. Gnidoi, A. Merzlyakov, A. Surenkov, V. Uglov, A. Zagnitko, V. Subbotin, I. Sannikov, A. Toropov, V. Afonichkin, A. Bovet, V. Khokhlov, V. Shishkin, M. Kormilitsyn, A. Lizin, and A. Osipenko.
Molten salt actinide recycler and transforming system without and with Th-U support: Fuel cycle flexibility and key material properties.
Annals of Nuclear Energy, 64(Supplement C):408–420, February 2014.

[7] Alexander Lindsay, Gavin Ridley, Andrei Rykhlevskii, and Kathryn Huff.
Introduction to Moltres: An application for simulation of Molten Salt Reactors.
Annals of Nuclear Energy, 114:530–540, April 2018.

[8] Gavin Ridley, Alexander Lindsay, and Kathryn Huff.
An Introduction to Moltres, an MSR Multiphysics Code.
In *Transactions of the American Nuclear Society*, Washington D.C., October 2017. American Nuclear Society.

[9] Aleksandr Obabko, Paul Fischer, Oana Marin, Elia Merzari, and Dave Pointer.
Verification and Validation of Nek5000 for T-junction, Matis, SIBERIA, and Max Experiments.
In *Proceedings of the 16th International Topical Meeting on Nuclear reactor Thermal-hydraulics, NURETH-16, Chicago, Illinois, August 30th-September 4th*, volume 2015, 2015.

References III

[10] Manuele Aufiero, Massimiliano Fratoni, and Pablo Rubiolo.
Monte Carlo/CFD Coupling for Accurate Modeling of the Delayed Neutron Precursors and Compressibility Effects in Molten Salt Reactors.
In *Transactions of the American Nuclear Society Annual Meeting*, volume 116, San Francisco, CA, June 2017. ANS.